RESEARCH PAPER

PCCP
www.rsc.org/pccp

Is the ESR spectrum attributable to H_2^- or $H_2^+(H_2)_2$? Precise measurement of the *g*-value and anisotropic hyperfine structure in γ-irradiated solid parahydrogen

Jun Kumagai,* Masatsugu Hanabusa, Hiroki Inagaki and Susumu Kariya

Department of Applied Chemistry, Graduate School of Engineering, Nagoya University, Fro-cho Chikusa-ku, Nagoya 464-8603, Japan. E-mail: kumagai@apchem.nagoya-u.ac.jp; Fax: +81-52-7892591; Tel: +81-52-7892591

Received 23rd February 2004, Accepted 2nd June 2004
First published as an Advance Article on the web 24th June 2004

Four ESR lines, found by Miyazaki *et al.* in 1995 in irradiated solid parahydrogen (*ca.* 92% para-purity) at 4.2 K, assigned as "H_2^-," were precisely re-measured with highly pure solid parahydrogen (>99.9%) and compared with calculated *g*-value and hyperfine coupling constants of $H_2^+(H_2)_2$. The *g*-value of $I,M_I = 0,0$ feature, reported previously as 2.0033 or 2.0023, was found to be incorrect and has now been corrected to 2.002120 ± 0.000012. This corrected value is clearly smaller than that of free electron. We also found that the remaining three lines corresponding to $I,M_I = 1,0$; 1, +1; and 1, –1 features have axially symmetric hyperfine anisotropic structure *i.e.*, $A_{\parallel} = 20.318$ and $A_{\perp} = 20.502$ mT. This anisotropy corresponds to the rotation of the species in solid parahydrogen. Although the experimental *g*-value and isotropic hyperfine coupling constants are in good agreement with those of $H_2^+(H_2)_2$ estimated by *ab initio* calculation, it is still difficult to explain why $H_2^+(H_2)_2$ clusters turned into ESR inactive species by addition of 0.1 ~ 1% D_2 in the present system. In this regard, we still maintain that the species in solid parahydrogen are H_2^-.

Introduction

Solid parahydrogen (*p*-H_2) molecules, which have a total nuclear spin $I = 0$ due to opposite nuclear spins in the individual H atoms in H_2 molecules, are one of the most extraordinary quantum solids that have demonstrated atomic tunneling reaction of H and H_2 and so on.[1] Solid *p*-H_2 is also a very useful matrix medium which enables ultra-high resolution spectroscopy of ESR and IR measurements identical to the resolutions of the spectra in the gas phase.[2–10]

In 1995, Miyazaki *et al.* found a very narrow isotropic doublet in the ESR spectrum in γ-irradiated solid *p*-H_2 at 4.2 K with a separation of 1.24 mT and a mid-point *g*-value of 2.007.[11] They designated the two signals temporally as radical pairs comprising trapped electrons and H_2^+ radicals. However, Symons pointed out that these novel lines might be due to a second order splitting of the $I,M_I = 1,0$ and 0,0 features.[12] The two ionic hydrogen species, H_2^+ and H_2^-, were considered as possibilities; of these, Symons suggested that the species was H_2^- anions. He assigned a real *g*-value of 2.0033 to the spectrum, and the ^{1}H-hyperfine splitting, estimated from the 1.24 mT, was 20.3 mT for two equivalent protons, so that the two outer lines due to $I,M_I = 1, \pm 1$ features could be predicted. In 1996, Kumada *et al.* found two broadened lines at ±20.3 mT from the line at $g = 2.0033$ as Symons had predicted, and four lines due to $I,M_I = 1,0$; 0,0; 1, ±1 features were denoted as B1 to B4, as shown in Fig. 1.[13] Since $I,M_I = 1, \pm 1$ species of a H_2^+ molecule, which was found in the gas phase, showed 28.7 mT in ^{1}H-hyperfine splitting,[14] the observed spectrum showed ^{1}H-hyperfine splitting of 20.3 mT, which was 30% smaller than that of 28.7 mT in H_2^+ cation molecules. This 30% reduction of ^{1}H-hyperfine splitting of H_2^+ molecules in solid phase is very difficult to explain. In addition, H_2^+ molecules have never been observed in solid hydrogen. When solid H_2 is exposed to ionizing radiations, H_2^+ and electrons are initially formed as an elementary process of radiation chemistry. The electrons can either be trapped in some way or returned to the H_2^+ to yield H_2 in an electronically excited state. These electrons may either return to the ground state or dissociate to release a pair of hydrogen atoms. Further, H_2^+ can react with H_2 to give H_3^+ and H atoms, which has been explained by the fast reaction, $H_2^+ + H_2 \rightarrow H_3^+ + H$ even at cryogenic temperatures.[15,16] By ESR measurements, Miyazaki *et al.* directly proved that H atoms are produced in γ-irradiated solid hydrogen at 4.2 K.[17–22] Based on these reasons, Symons initially indicated that the B1 to B4 lines were probably due to the H_2^- anion molecules. Ichikawa *et al.* proposed a few formation mechanisms of H_2^- and electron bubbles in solid hydrogen.[23,24]

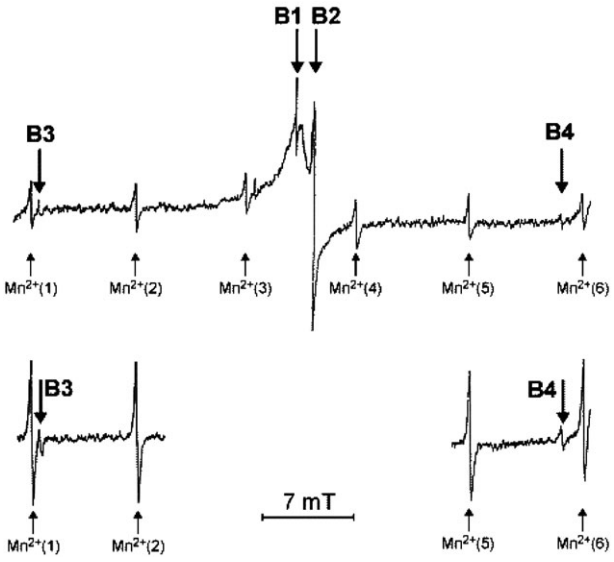

Fig. 1 ESR spectra at 4.2 K in γ-irradiated solid *p*-H_2 reported by Kumada *et al.* in 1996.[13] Lines B1, B3, and B4 have been assigned as *ortho*-H_2^- and line B2 as *para*-H_2^-, respectively.

DOI: 10.1039/b402756f

However, a major unresolved problem is that the *g*-value of 2.0033 for $I,M_I = 0,0$ feature is larger than that of free electron. Bruna *et al.* calculated the *g*-value shift (Δg) of H_2^- and H_2^+ ion molecules from that of free electron (2.002319) by their established method and concluded that both of them should have negative Δg-values.[25] They suggested that a positive *g*-shift implies an increase in the effective angular momentum relative to the free electron; however, it is difficult to understand how this might be achieved by $H_2^-(\sigma_g^2\,\sigma_u)$. Further, they also mentioned that large positive *g*-shifts have been measured for other $^2\sigma_u^+$ radicals such as F_2^- and Cl_2^-. In 2000, Symons and Woolley suggested that the radical center is H_2^+ rather than H_2^-, as previously suggested, because the *g*-value of 2.0033 given by Symons and Miyazaki for narrow $I,M_I = 0,0$ feature (B2 line) is greater than the free electron *g*-value, whereas it should be less for H_2^-.[26] They performed electronic structure calculations for a range of cluster structures to simulate the local environment of both radicals in a hydrogen matrix. No stable structure was found for the anion clusters, whereas H_2^+ remained strongly bonded with extensive delocalization onto neighboring H_2 molecules. The extent of delocalization (*ca.* 30%) closely agreed with the expectation of reduction in ^{1}H-hyperfine splitting from 28.7 to 20.3 mT. In 2001, Suter *et al.* performed *ab initio* calculation based on the density functional theory (DFT) for $H_6^{\pm}$ and $H_{14}^{\pm}$ clusters in order to simulate ^{1}H-hyperfine constants. They found that isotropic hyperfine coupling constants in a H_6^+ were approximately 572 MHz (= 20.4 mT) and in excellent agreement with the experimental value reported by Kumada *et al.*[27] Chan *et al.* reported an infrared spectrum of *p*-H_2 crystals ionized by 3 MeV electrons and found five lines, which they assigned to $H_3^+(H_2)_n$ and $H^-(H_2)_n$.[16] Further, they indicated that electron bubbles and H_2^- molecules were never stable for a long time, such as several hours, in the *p*-H_2 crystal.

Although most of the researches have yielded negative results for the existence of H_2^- molecules in solid *p*-H_2, a few questions still need to be answered. Firstly, theoretical treatments of hydrogen ion radicals or excess electrons are not enough for discussing their stability in solid hydrogen. With regard to the solvation of excess electrons in $(benzene)_n^-$ and $(toluene)_n^-$ clusters, Mitsui *et al.* found that very large coordination numbers ($n \sim 25$) are necessary for the formation of stable benzene and toluene cluster anions.[28] Recently, they observed similar results in $(CH_3CN))_n^-$ clusters.[29] These results indicate that very large coordination numbers of hydrogen clusters should be considered for discussing excess electrons or $H_2^{\pm}$ molecules in solid hydrogen. Secondly, yields of B1 to B4 lines increased when small amounts of helium contaminated a solid *p*-H_2 crystal;[1] their yields were very low in the absence of helium. This indicates that the species due to B1 to B4 lines could be generated in defects or vacancies of solid *p*-H_2. Thirdly, the *g*-value of 2.0033 for $I,M_I = 0,0$ feature (B2 line) is probably incorrect. In 1995, when Miyazaki *et al.* measured the ESR spectrum of doublet lines (B1 and B2), they did not use any microwave frequency counters. Only the third and fourth lines of Mn^{2+} in MgO were used as the *g*-value standard in the conventional method, which is a less reliable way of measurement for obtaining a precise *g*-value. Miyazaki *et al.* thought that the doublet lines originated from hyperfine interaction of radical pairs comprising trapped electrons and H_2^+ radicals having 1.24 mT of hyperfine constants. Hence, they thought that the midpoint of B1 and B2 lines corresponded to the *g*-value of the species. The *g*-value of 2.0033 for $I,M_I = 0,0$ feature (B2 line) was derived by Symons at a (=half of hyperfine constant of 1.24 mT) higher magnetic field of 0.62 mT from the midpoint of B1 and B2 lines, so that the *g*-value of 2.0033 also has a low degree of accuracy. In spite of Ichikawa *et al.* correcting the *g*-value to 2.0023 in their previous paper,[23] this value is not precise enough for conducting further discussion.

Recently, we succeeded in improving the purity of *p*-H_2 contents in solid hydrogen to 99.9%. This was done by converting the remaining orthohydrogen (*o*-H_2) to *p*-H_2 using FeO(OH) as *ortho–para* converting catalyst in liquid H_2 at 14 K, which led to several important findings in ultra-high resolved ESR spectroscopy.[1,4,30,31] In this study, we have re-measured B1 to B4 lines in very pure solid *p*-H_2 containing 0.1% helium. We succeeded in observing a very sharp and isotropic spectrum for B2 line ($\Delta H_{msl} \sim 0.006$ mT) and axially symmetric hyperfine anisotropic structure in B1, B3, and B4 lines. These highly resolved ESR spectra are desirable for precise analysis and will serve as important data for the discussion on the assignment of B1–B4 lines and whether these are attributable to H_6^+ or H_2^-.

The objectives of this study are as follows: (i) to determine whether the species for B1–B4 lines are H_6^+ or H_2^- by precise measurement of *g*-value of B2 line and by theoretical calculation of *g*-value; (ii) to precisely analyze the anisotropic structures in B1, B3, and B4 lines using the Breit–Rabi equation[32,33] and discuss the rotational motion of the species.

For *g*-marker of B2 line, we chose a perylene radical cation in sulfuric acid, which has a *g*-value of 2.002583 at the central line with a very sharp linewidth of *ca.* 0.015 mT. Due to the spectrum line width of B2 signals such as 0.006 mT, conventional *g*-marker sample such as DPPH are insufficient owing to the broad line width of 0.1 mT. We simultaneously measured the B2 line and the signal of perylene radical cation by inserting the perylene sample into the ESR cavity from the reference hole, which enabled us to accurately compare their resonant magnetic fields.

Experimental

Sample preparation

Parahydrogen (*p*-H_2) was produced by immersing powdered iron hydroxide (FeO(OH)) into liquid normal hydrogen (99.9999%), which contained 75% *ortho*-H_2 (*o*-H_2) at 14 K for a total duration of more than 10 h.[4,30,31] The concentration of *p*-H_2 reached approximately 99.9%. Helium at 0.1% was added to all the samples in order to increase the yields of B1 to B4 lines.[1] The gaseous hydrogen of each sample was sealed in a quartz ESR tube and solidified by immersing the sample tube into a quartz Dewar filled with liquid helium. The solid hydrogen sample was γ-irradiated at 4.2 K with a dose of 0.72 kGy at the ^{60}Co γ-ray radiation facility at Nagoya University, Japan.

ESR measurement

The ESR spectra of the irradiated samples at 4.2 K were measured by a JES-RE1X ESR spectrometer (JEOL). In order to avoid spectrum broadening due to large modulations, field modulation frequency and width for ESR measurements were chosen as 50 kHz and 0.005 mT, respectively. Microwave powers for avoiding saturation of spectra in ESR measurements are 0.1, 0.001, 1, and 1 mW for B1, B2, B3, and B4 lines, respectively. Microwave frequencies were monitored by the 53150A microwave frequency counter (Hewlett-Packard). Sweep width of magnetic fields were calibrated by the EFM-2000AX NMR field meter (Echo Electronics Co. Ltd.). Precise magnetic field at the irradiated *p*-H_2 sample in the ESR cavity was determined by measuring perylene radical cation in 0.96 mM of perylene in sulfuric acid. A capillary tube with the perylene sample was inserted into the JEOL ESR cavity from the reference hole, and the B2 line and the perylene radical cation signals were measured simultaneously. The *g*-value of perylene radical cation in sulfuric acid was precisely analyzed by Segal *et al.*, and its value was reported as 2.002578.[34] This value was observed by correcting the second order shift of the signal by ^{1}H-hyperfine coupling constant of

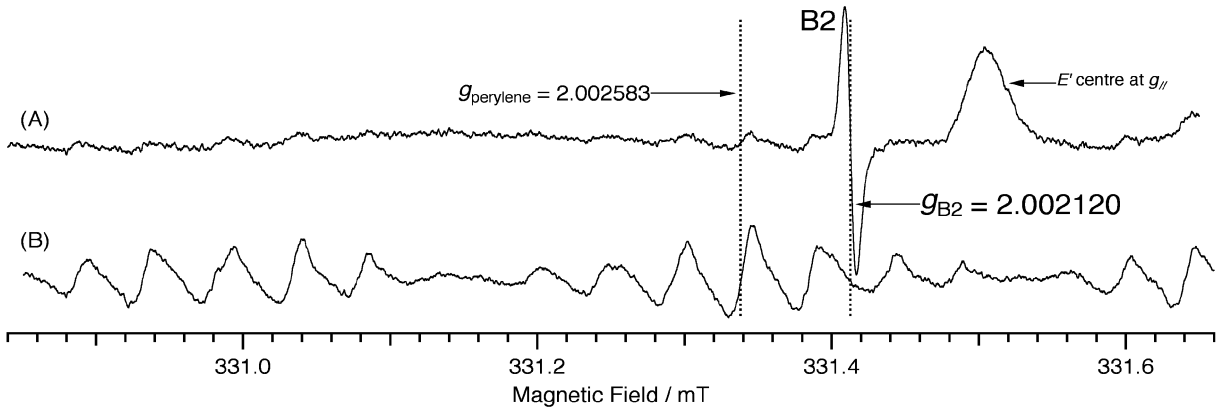

Fig. 2 ESR spectra at 4.2 K in (A) γ-irradiated solid parahydrogen (99.9%) with He (0.1%), which was measured with perylene radical cation in 0.96 mM perylene in sulfuric acid in a capillary tube at room temperature inserted from a reference hole of JEOL ESR cavity; (B) the perylene radical cation in 0.96 mM perylene in sulfuric acid at room temperature, which was the sample solution, located in the center of the cavity. The phase of the spectrum (B) is inversed for the purpose of comparison with spectrum (A). Microwave power, frequency, field modulation frequency, and width for the measurement of spectrum (A) are 0.1 mW, 9.292100 GHz, 50 kHz, and 0.005 mT, respectively. Maximum slope line widths (ΔH_{msl}) of B2 line and central line of perylene radical cation are 0.006 and 0.015 mT, respectively. The vertical dotted lines indicate the center of the spectrum of B2 line and perylene radical cation signal at g = 2.002120 and 2.002583, respectively. B2 line has been assigned as H_2^- molecule of $I,M_I = 0,0$ feature. Broad line at the higher magnetic field of B2 line is due to E' center at $g_{\|}$ of the Suprasil quartz tube made by γ-irradiation.

perylene radical cation. We used an uncorrected g-value of 2.002583 at the center of the signal of perylene radical cation in order to provide an absolute magnetic field from the center of the signal. Samples of the perylene radical cation or DPPH were used as standards because the field meter had a small offset value for the measured magnetic field.

Results

g-Value of I,M_I = 0,0 feature (B2 line)

Fig. 2A shows the ESR spectrum of B2 line at 4.2 K for γ-irradiated p-H_2 with multiplet lines due to perylene radical cation in 0.96 mM perylene in sulfuric acid in the capillary tube at room temperature inserted from a reference hole of the ESR cavity. This is the reason for the inversion of the signal phase of perylene radical cation. The ESR spectrum of only perylene radical cation is also shown in Fig. 2B in an inversed phase. The center of multiplet lines due to perylene radical cation has a g-value of 2.002583;[34] magnetic field of the central line is obtained as 331.6016 ± 0.0019 mT for a microwave frequency of 9.292100 GHz. Thus, the g-value in the center of B2 line, which corresponds to I,M_I = 0,0 feature, is observed to be 2.002120 ± 0.000012 (average of eight measurements) for a difference in magnetic field of 0.0767 mT from the centre of perylene radical cation. The g-value of B2 line is significantly smaller than that of free electron (g_e = 2.002319).

Anisotropic hyperfine structure

Fig. 3 shows the ESR spectra of B1–B4 lines for γ-irradiated p-H_2 at 4.2 K in solid lines and simulated spectra provided by Breit–Rabi equation in dotted lines. Although only B2 line shows an isotropic shape, B1, B3, and B4 lines, which correspond to I,M_I = 1,0; 1, +1; and 1, −1, respectively, show anisotropic structures that are clearly observed in this study due to the increase in purity of p-H_2.

Previously, the second order perturbation theory was used to explain the separated resonant fields of B1 and B2 lines, I,M_I = 1,0 and 0,0 features, respectively, and this approximately satisfied the conditions for determining the old experimental data.[13] In this study, we applied the Breit–Rabi equation instead of the second order perturbation theory because the former can provide a precise solution for shifts of B1, B3, and B4 lines due to the large value of hyperfine coupling

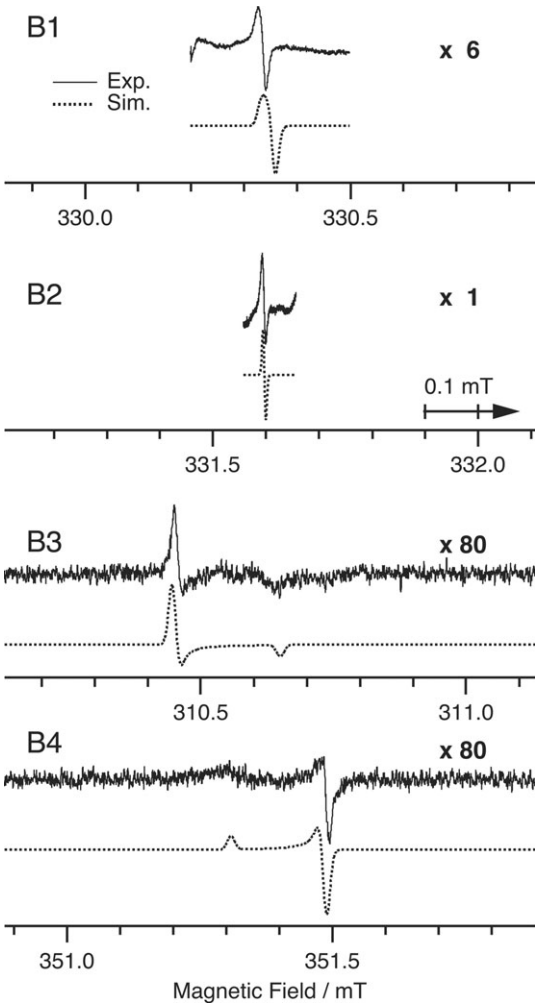

Fig. 3 ESR spectra of B1–B4 lines for γ-irradiated p-H_2 at 4.2 K (solid lines) and simulated spectra provided by Breit–Rabi equation (dotted lines) using the following parameters: g = 2.002120, $A_{\|}$ = 20.318 mT, and $A_{\perp}$ = 20.502 mT. Intensities of the observed spectra are normalized by dividing with the square root of applied microwave power for their measurements. Microwave frequencies in each spectrum are normalized at 9.292120 GHz. A gaussian line shape with 0.015 mT line width was applied for the simulation of B1, B3, and B4 lines.

Table 1 Experimental *g*-value and isotropic hyperfine coupling constants observed by analysis of B1–B4 lines and calculated *g*-value and constants corresponding to $H_2^+(H_2)_2$ optimized structure

	g-Value	Isotropic hyperfine coupling constants/mT
Exp.	2.002120 ± 0.000012 (measured 8 times)	20.438 ($A_\parallel$ = 20.318, $A_\perp$ = 20.502)
$H_2^+(H_2)_2$[a]	2.002238	20.09 (center H_2^+) 10.21 (outer two H_2)

[a] Calculated by Gaussian 03 with basis set of B3LYP/6-311++G (3df,3pd). The structure of $H_2^+(H_2)_2$ applied to the calculation is shown in Scheme 1 and is the same as that proposed by Symons *et al.*[26]

constant.[32,33] The best ESR parameters for fitting the observed spectra are listed in Table 1. The method for determining an isotropic hyperfine coupling constant (A_f) from experimental value is described in the Discussion section. Optimized structure, calculated *g*-value, and isotropic hyperfine coupling constant of $H_2^+(H_2)_2$, obtained from Gaussian 03 with B3LYP/6-311 ++G(3df,3pd) level, are shown in Scheme 1 and listed in Table 1 for the purpose of comparison.[35] The structure of $H_2^+(H_2)_2$ applied for the calculation is the same as that proposed by Symons *et al.*[26] As shown in Table 1, the observed and calculated *g*-value and hyperfine couplings are in good agreement with each other. Although hyperfine coupling constants have a value of 10.21 mT for two outer H_2 in $H_2^+(H_2)_2$, they will not appear in the spectrum if both H_2 are parahydrogen.

Discussion

ESR parameters for B1 to B4 lines

***g*-value of I,M_I = 0,0 feature (B2 line).** In this study, we observed the precise experimental *g*-value of $I,M_I = 0,0$ feature (B2 line) to be 2.002120, which is smaller than that of free electron. The value of 2.0033, provided by Symons and Miyazaki, was completely incorrect.[11,12] Ichikawa *et al.* revised the *g*-value to 2.0023 in 1998; however, even this value was not accurate.[24] Our precise assignment of *g*-value at B2 line was realized by increasing *para*-contents in solid hydrogen and using perylene cation sample as a *g*-value standard. In their studies, both Symons *et al.* and Bruna *et al.* pointed out that H_2^- species should show smaller *g*-value compared to that of free electron (2.002319).[25,26,36,37]

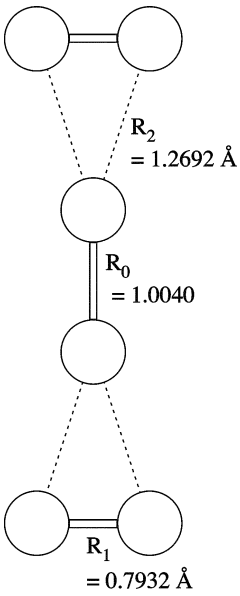

Scheme 1 Schematic representation of optimized structure of $H_2^+(H_2)_2$ calculated by Gaussian 03 with B3LYP/6-311++G(3df,3pd) level.

We did not expect that the calculated *g*-value of $H_2^+(H_2)_2$ would be negative compared to that of free electron, which counters the claims of Symons. He expected that the *g*-value of $H_2^+(H_2)_2$ would be positive compared to that of free electron because the delocalization of hole of H_2^+ to the surrounding H_2 matrix molecules could induce admixtures of 2p(π) orbitals giving a positive shift. It is well known[37–40] that Δg can be written in deformed form as

$$\Delta g = \Delta g_{\mathrm{RMC\text{-}SZ}} + \Delta g_{\mathrm{GC\text{-}SZ}} + \Delta g_{2\mathrm{O}} \quad (1)$$

where $\Delta g_{\mathrm{RMC\text{-}SZ}}$, $\Delta g_{\mathrm{GC\text{-}SZ}}$, and $\Delta g_{2\mathrm{O}}$ are spin-Zeeman relativistic mass correction term, spin-Zeeman gauge correction term, and second order term including spin–orbit coupling and orbit-Zeeman interaction, respectively. The spin-Zeeman relativistic mass correction term depends on the density of the unpaired electron near the nuclei. This term becomes negative when the SOMO becomes more compact, leading to an increase in the kinetic energy of the unpaired electrons. The spin-Zeeman gauge correction term is related to the electron–nuclear Coulomb attraction as a positive shift and electron–electron repulsion as a negative shift. The second order term including spin–orbit coupling and orbit–Zeeman interactions is inversely proportional to the excitation energy between the ground and excited states. In case of H_2^+, $\Delta g_{\mathrm{RMC\text{-}SZ}}$ and $\Delta g_{\mathrm{GC\text{-}SZ}}$ were estimated as −64 and +22 ppm, respectively,[37] and $\Delta g_{2\mathrm{O}}$ was negligibly small. In the case of $H_2^+(H_2)_2$, the $\Delta g_{2\mathrm{O}}$ term was not negligible and induced a positive shift through delocalization of unpaired electron to outer two H_2 molecules as Symons had indicated.[26] An H_2 molecule in the center and two H_2 molecules on outer side were estimated to have unpaired spin densities corresponding to 20.09 and 10.21 mT, respectively, which provide a larger negative shift of $\Delta g_{\mathrm{RMC\text{-}SZ}}$ and may overcome the positive shift of $\Delta g_{2\mathrm{O}}$. In case of H_2^-, $\Delta g_{\mathrm{RMC\text{-}SZ}}$ term may be the same as that of center H_2 in $H_2^+(H_2)_2$. $\Delta g_{\mathrm{GC\text{-}SZ}}$ term will shift to negative due to electron–electron repulsion, and $\Delta g_{2\mathrm{O}}$ term may be negligibly small. Thus, the experimental *g*-value of 2.002120 is adequate for either $H_2^+(H_2)_2$ or H_2^-.

Hyperfine coupling constants and their anisotropy in I,M_I = 1,0; 1, +1; and 1, −1 features (B1, B3 and B4 lines)

Rotation of the species in solid parahydrogen at 4.2 K by analysis of anisotropy in I,M_I = 1,0; 1, +1; and 1, −1 features (B1, B3 and B4 lines). As shown in Fig. 3 and Table 1, B1, B3 and B4 lines have clear axial symmetric anisotropy in their spectra; however, the appearance of the anisotropy is unusual. Assuming H–H bond of H_2 ion as the *z*-axis and the center of the bond as the origin of axes, both *x*- and *y*-axes are perpendicular to the *z*-axis as shown in Scheme 2. When H_2 ions are in a rigid state in solid *p*-H_2, $A_\parallel$ and $A_\perp$ can be expressed as follows:

$$A_{zz} = |A_f + 2A_\mathrm{d}|,\ A_{xx} = A_{yy} = |A_f - A_\mathrm{d}| \quad (2)$$

$$A_\parallel = A_{zz} = |A_f + 2A_\mathrm{d}| \quad (3)$$

$$A_\perp = (A_{xx} + A_{yy})/2 = |A_f - A_\mathrm{d}|, \quad (4)$$

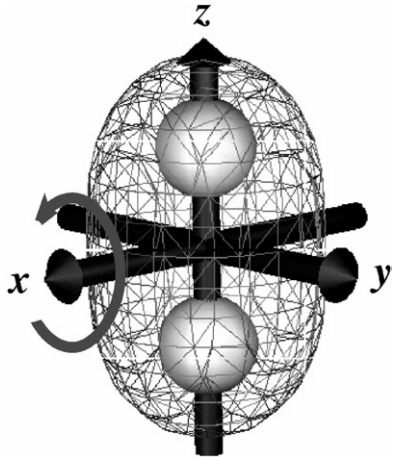

Scheme 2 Schematic representation of coordinates and rotation of H_2 ion in solid parahydrogen at 4.2 K.

where A_f and A_d are hyperfine coupling constants due to Fermi contact term and magnetic dipole–dipole interaction, respectively. $A_{\|}$ should be larger than $A_{\perp}$ if H_2 ions are fixed in solid hydrogen in random orientation; however, observed spectra clearly showed that $A_{\|}$ is smaller than $A_{\perp}$. This opposite appearance of anisotropic hyperfine coupling constants can be explained by the model in which H_2 ions rotate rapidly around the x-axis (or y-axis) in solid p-H_2, such that they average out the associated hyperfine anisotropy. The $A_{\|}$ and $A_{\perp}$ can be expressed as

$$A_{\|} = A_{xx} = |A_f - A_d| \quad (5)$$

$$A_{\perp} = (A_{yy} + A_{zz})/2 = |A_f + A_d/2| \quad (6)$$

by averaging A_{yy} and A_{zz} rotating around the x-axis. Thus, the experimental fact that $A_{\|} < A_{\perp}$ can be explained by the rotation of H_2 ions around the x-axis in solid p-H_2 at 4.2 K. The observed values of A_f and A_d from eqns. (5) and (6) are as 20.438 and 0.167 mT, respectively.

Value of isotropic hyperfine coupling constants. The observed isotropic hyperfine coupling constant, which has a value of 20.438 mT, is almost 30% smaller than that of H_2^+ in the gas phase, which has a value of 28.7 mT. Isotropic hyperfine coupling constant of $H_2^+(H_2)_2$ in central o-H_2^+ was calculated as 20.1 mT in this study, and Suter *et al.* also observed a similar value of 20.4 mT.[27] Although ESR parameters of $I,M_I = 1,0$; 1, +1; and 1, −1 features suitably satisfy the assignment as o-$H_2^+(p\text{-}H_2)_2$, they also satisfy the assignment as o-H_2^-. The isotropic hyperfine coupling of o-H_2^- is expected to be lower than that of o-H_2^+. If the unpaired electron of o-H_2^- is accommodated in an antibonding σ* orbital, its spin density at nuclei is lower than that of σ orbital, resulting in reduction of the constant. Isotropic hyperfine coupling constants of $H_2^+(H_2)_2$ in outer H_2 molecules were estimated as 10.21 mT, as shown in Table 1. If one or two outer H_2 molecules of $H_2^+(H_2)_2$ are orthohydrogens, further hyperfine splitting should be visible in the observed spectra. Since we used highly pure *para*-hydrogen, the outer H_2 molecules are p-H_2 which resulted in no further hyperfine splitting in the observed spectra. The ESR spectra never exhibited further hyperfine splitting when o-H_2 was mixed in the range of 0.1 to 10%. The fact that $I,M_I = 1,0$; 1, +1; and 1, −1 features can be observed when solid p-H_2 (99.9%) was irradiated is rather strange and noteworthy. It could be explained that H_2 molecules may be excited at higher rotational level with nuclear spin being converted from p-H_2 to o-H_2 when H_2 molecules are ionized or reduced by ionizing radiation and/or attachment of electrons, respectively.

Which is more probable—the existence of H_2^- or $H_2^+(H_2)_2$—in solid *para*-hydrogen?

The g-value and isotropic hyperfine coupling constants of B1 to B4 lines are consistent with those of $H_2^+(H_2)_2$, as expected by the *ab-initio* calculation and well illustrated in Table 1. Two mechanisms have been proposed for the formation of $H_2^+(H_2)_2$. Full dimensional *ab initio* direct dynamics calculations of the ionization of clusters $H_2(H_2)_n$ ($n = 3$, 4, and 6) were performed by Tachikawa.[41] He concluded that ionized H_2^+ molecule approached the neighboring H_2 molecules in approximately 100 fs, and reacted as

$$H_2^+ + H_2 \rightarrow H_3^+ + H \quad (7)$$

within 10 to 20 fs. He pointed out that $H_2^+(H_2)$ and $H_2^+(H_2)_2$ clusters can exist in a stable form if the excess energy of H_2^+ is rapidly and efficiently removed from the complexes to bath-relaxation modes of the solid hydrogen. Since intensities of the B1 to B4 lines increased when a small amount of He or Ne, such as ∼0.1 mol%, were mixed in solid p-H_2,[1] they can serve as good energy absorbers for excited H_2^+. Kurosaki and Takayanagi carried out *ab initio* molecular orbital calculations for the H_6^+ cluster and found two isomers as $H(H_3^+)H_2$ and $H_2^+(H_2)_2$ and a transition state (TS) for direct isomerization.[42] The TS is located at the saddle point of the isomerization path. If their model can be applied to the solid phase, thermalization of H_2^+ would not be required for the formation of $H_2^+(H_2)_2$. Since H and H_3^+ are the major products in irradiated solid hydrogen, the pre-isomer of $H(H_3^+)H_2$ can be formed. $H(H_3^+)H_2$ and $H_2^+(H_2)_2$ were estimated to be 45.5 and 49.5 kcal mol^{-1} lower than the $H_2^+ + 2H_2$ energy level, respectively.

The decay behavior of B1 or B2 lines has been studied by Kumada *et al.* as functions of temperature and concentration of o-H_2, HD, and D_2. Their half-lifetimes are *ca.* 150 to 250 min in solid p-H_2 at 4.2 K. Considering the decay process of $H_2^+(H_2)_2$, two possibilities can be proposed when $H_2^+(H_2)_2$ turns to ESR inactive species, as shown in the following reactions:

$$H_2^+(H_2)_2 \rightarrow H_3^+ + H_2 + H \quad (8)$$

$$H_2^+(H_2)_2 + H \rightarrow H_3^+ + 2H_2 + H. \quad (9)$$

Self-decomposition of $H_2^+(H_2)_2$ by reaction (8) does not proceed because reaction (7) is exothermic in 40 kcal mol^{-1}.[16] Since the energy level of $H_2^+(H_2)_2$ was estimated to be 49.5 kcal mol^{-1} lower than that of $H_2^+ + 2H_2$, the energy levels on both sides in reaction (8) may either be almost equal or slightly endothermic. In the case of reaction (9), this could be the possible mechanism for the decay of B1 or B2 lines. H atoms are the major products in irradiated solid hydrogen similar to H_3^+. Kumada *et al.* reported that diffusion of H atoms in solid hydrogen *via* $H + H_2 \rightarrow H_2 + H$ tunneling reaction is faster when the concentration of o-H_2 is lower.[31] Since the concentration of H atoms must be over 10^4 times larger than that of B1–B4 species,[11] reaction (9) should proceed as pseudo-first-order reaction kinetics. This is consistent with the decay analysis of B1 or B2 lines, as reported by Kumada *et al.*[43] Decay rates of B1 or B2 lines are slower when the concentration of o-H_2 is higher,[43] which corresponds to the observation that diffusion rates of H atoms are slower when the concentration of o-H_2 is higher.

Although the above discussion positively supports the existence of $H_2^+(H_2)_2$ in irradiated solid hydrogen, one issue still remains unresolved. When 0.1% D_2 was mixed with p-H_2, decay rates of B1 or B2 lines are *ca.* 10 times larger than those in absence of D_2. When the concentration is increased to over 1%, neither B1 nor B2 lines could be measured, and a singlet line assigned as electron bubble appeared.[44] If we assume that B1 and B2 lines are due to $H_2^+(H_2)_2$, the following question

arises. Why did the signals due to $H_2^+(H_2)_2$ decay faster when D_2 was mixed in solid *p*-H_2? Since $H_2^+(H_2)_2$ was estimated to be 49.5 kcal mol^{-1} lower than the $H_2^+ + 2H_2$ energy level, only 0.1% or 1% D_2 molecules in solid *p*-H_2 are likely to have no effect in breaking the $H_2^+(H_2)_2$ complex. The half-decay time of the singlet line assigned as electron bubble was approximately 200 min, which is almost 7 times slower than that of B1 or B2 lines when D_2 was added at 0.1%. Thus, the reaction

$$H_2^+(H_2)_2 + e_{bubble}^- \rightarrow 3H_2 \qquad (10)$$

is not consistent with the different decay rates. Therefore, it is extremely difficult to explain why $H_2^+(H_2)_2$ decayed faster when D_2 was mixed. In addition, if the isomerization of $H(H_3^+)H_2$ is a major process in producing $H_2^+(H_2)_2$ in solid hydrogen, yields of $H_2^+(H_2)_2$ should be independent of He concentration because H_3^+ and H are the major products in pure solid hydrogen. If this mechanism cannot be applied, H_2^+ molecules excited by ionizing radiations must be thermalized for formation of $H_2^+(H_2)_2$. This suggests that hot H_2^+ ion approaches two H_2 molecules equivalently, simultaneously removing the excess energy which stabilizes the clusters. Although He can be a good absorber of the excess energy, the formation of $H_2^+(H_2)_2$ would be rare due to the fast process of reaction (7), resulting in very low yields of H_2^+ or $H_2^+(H_2)_2$. This is consistent with the fact that H_2^+ has never been measured in solid hydrogen by any spectroscopic methods. Although the measurements of ion cluster of $H_3^+(H_2)_n$ or $H^-(H_2)_n$ in solid *p*-H_2 have been reported,[3] H_2^+ or $H_2^+(H_2)_n$ clusters have never been found to date.

Miyazaki has proposed that B1–B4 lines are due to H_2^-. Although the stable structure of H_2^- cannot be determined by *ab initio* calculation, the decay behavior of B1 and B2 lines can be clearly explained by his model, which suggests that H_2^- diffuses by tunneling through solid hydrogen and changes into electron bubbles at the D_2 sites.[43,45] The theoretical possibility of this model was discussed by Ichikawa *et al.*[24]

Conclusion

We found that the *g*-value of the species is smaller than that of free electron and that the species are rotating in solid *p*-H_2 at 4.2 K. Although the experimental *g*-value and isotropic hyperfine coupling constants are in good agreement with those of $H_2^+(H_2)_2$, it is still difficult to explain why $H_2^+(H_2)_2$ clusters turned into ESR inactive species by addition of $0.1 \sim 1\%$ D_2 to the present system. In this regard, we still maintain that the species are H_2^- in solid *p*-H_2. Further experimental data and theoretical treatment for solid phase are essential for developing this study.

Acknowledgements

This study is supported in part by grants from Ministry of Education, Science, Sports and Culture, Japan. We thank Dr Hiroto Tachikawa for providing the results of *ab initio* calculation of $H_2^+(H_2)_2$ and for the beneficial discussion. We also thank Dr Kenji Komaguchi for the valuable discussion on the analysis of anisotropic hyperfine structure.

References

1 *Atom Tunneling Phenomena, Physics Chemistry and Biology*, ed. T. Miyazaki, Springer-Verlag, Berlin, Heidelberg, NewYork, 2004.
2 D. T. Anderson, R. J. Hinde, S. Tam and M. E. Fajardo, *J. Chem. Phys.*, 2002, **116**, 594.
3 T. Momose, C. M. Lindsay, Y. Zhang and T. Oka, *Phys. Rev. Lett.*, 2001, **86**, 4795.
4 T. Kumada, J. Kumagai and T. Miyazaki, *J. Chem. Phys.*, 2001, **114**, 10024.
5 N. Sogoshi, Y. Kato, T. Wakabayashi, T. Momose, S. Tam, M. E. DeRose and M. E. Fajardo, *J. Phys. Chem. A*, 2000, **104**, 3733.
6 T. Momose, Y. Zhang and T. Oka, *Physica B*, 2000, **284**, 387.
7 Y. Zhang, T. J. Byers, M. C. Chan, T. Momose, K. E. Kerr, D. P. Weliky and T. Oka, *Phys. Rev. B*, 1998, **58**, 218.
8 R. M. Dickson, T. Momose, T. J. Byers and T. Oka, *Phys. Rev. B*, 1998, **57**, 941.
9 T. Momose, M. Miki, T. Wakabayashi, T. Shida, M. C. Chan, S. S. Lee and T. Oka, *J. Chem. Phys.*, 1997, **107**, 7707.
10 D. P. Weliky, K. E. Kerr, T. J. Byers, Y. Zhang, T. Momose and T. Oka, *J. Chem. Phys.*, 1996, **105**, 4461.
11 T. Miyazaki, K. Yamamoto and Y. Aratono, *Chem. Phys. Lett.*, 1995, **232**, 229.
12 M. C. R. Symons, *Chem. Phys. Lett.*, 1995, **247**, 607.
13 T. Kumada, H. Inagaki, T. Nagasawa, Y. Aratono and T. Miyazaki, *Chem. Phys. Lett.*, 1996, **251**, 219.
14 A. Carrington, I. R. Mcnab and C. A. Montgomerie, *J. Phys. B.*, 1989, **22**, 3551.
15 T. Oka, *Ann. Rev. Phys. Chem.*, 1993, **44**, 299.
16 M. C. Chan, M. Okumura and T. Oka, *J. Phys. Chem. A*, 2000, **104**, 3775.
17 T. Miyazaki, N. Iwata, K. Fueki and H. Hase, *J. Phys. Chem.*, 1990, **94**, 1702.
18 T. Miyazaki, M. Kato and K. Fueki, *Radiat. Phys. Chem.*, 1990, **36**, 501.
19 T. Miyazaki, N. Iwata, K. P. Lee and K. Fueki, *J. Phys. Chem.*, 1989, **93**, 3352.
20 T. Miyazaki and K. P. Lee, *J. Phys. Chem.*, 1986, **90**, 400.
21 T. Miyazaki, *Bull. Chem. Soc. Jpn.*, 1985, **58**, 2413.
22 T. Miyazaki, H. Tsuruta and K. Fueki, *J. Phys. Chem.*, 1983, **87**, 1611.
23 T. Ichikawa, H. Tachikawa, J. Kumagai, T. Kumada and T. Miyazaki, *J. Phys. Chem. A*, 1997, **101**, 7315.
24 T. Ichikawa, H. Tachikawa, T. Kumada, J. Kumagai and T. Miyazaki, *Chem. Phys. Lett.*, 1999, **307**, 283.
25 P. J. Bruna, G. H. Lushington and F. Grein, *Chem. Phys. Lett.*, 1996, **258**, 427.
26 M. C. R. Symons and R. G. Woolley, *Phys. Chem. Chem. Phys.*, 2000, **2**, 217.
27 H. U. Suter, B. Engels and S. Lunell, *Adv. Quantum Chem.*, 2001, **40**, 133.
28 M. Mitsui, A. Nakajima and K. Kaya, *J. Chem. Phys.*, 2002, **117**, 9740.
29 M. Mitsui, N. Ando, S. Kokubo, A. Nakajima and K. Kaya, *Phys. Rev. Lett.*, 2003, **91**.
30 T. Miyazaki, H. Fukuta, M. Hanabusa, T. Kumada and J. Kumagai, *Chem. Phys. Lett.*, 2002, **360**, 8.
31 T. Kumada, M. Sakakibara, T. Nagasaka, H. Fukuta, J. Kumagai and T. Miyazaki, *J. Chem. Phys.*, 2002, **116**, 1109.
32 J. E. Nafe and E. B. Nelson, *Phys. Rev.*, 1948, **73**, 1948.
33 G. Breit and I. I. Rabi, *Phys. Rev.*, 1931, **38**, 2082.
34 B. G. Segal, M. Kaplan and G. K. Fraenkel, *J. Chem. Phys.*, 1965, **43**, 4191.
35 H. Tachikawa, *Ab initio* calculation of *g*-value of H_6^+, personal communication.
36 P. J. Bruna and F. Grein, *Int. J. Quantum Chem.*, 2002, **90** 472.
37 G. H. Lushington, P. J. Bruna and F. Grein, *Int. J. Quantum Chem.*, 1997, **63**, 511.
38 R. Angstl, *Chem. Phys.*, 1989, **132**, 435.
39 R. McWeeny, *Methods of Molecular Quantum Mechanics (Theoretical Chemistry)*, Academic Press, London, 1992.
40 F. Neese, *J. Chem. Phys.*, 2001, **115**, 11080.
41 H. Tachikawa, *Phys. Chem. Chem. Phys.*, 2000, **2**, 4702.
42 Y. Kurosaki and T. Takayanagi, *Chem. Phys. Lett.*, 1998 **293**, 59.
43 T. Kumada, N. Kitagawa, S. Mori, J. Kumagai, Y. Aratono and T. Miyazaki, *J. Low Temp. Phys.*, 1999, **114**, 413.
44 T. Kumada, S. Mori, J. Kumagai, Y. Aratono and T. Miyazaki, *J. Phys. Chem. A*, 1999, **103**, 8966.
45 T. Miyazaki, *Adv. Quantum Chem.*, 2003, **43**, 217.

